

Distribution Agreement

In presenting this thesis as a partial fulfillment of the requirements for a degree from Emory University, I hereby grant to Emory University and its agents the non-exclusive license to archive, make accessible, and display my thesis in whole or in part in all forms of media, now or hereafter known, including display on the world wide web. I understand that I may select some access restrictions as part of the online submission of this thesis. I retain all ownership rights to the copyright of the thesis. I also retain the right to use in future works (such as articles or books) all or part of this thesis.

Signature:

Sara Lykken

April 14, 2010

Harmonics Echoing Across Time and Space:
A Summary of Research on the Topology of the Universe

By

Sara Lykken

Advisers: Emily Hamilton and David Borthwick

Department of Mathematics and Computer Science

Emily Hamilton
Adviser

David Borthwick
Adviser

Monica Capra
Committee Member

April 14, 2010

Harmonics Echoing Across Time and Space:
A Summary of Research on the Topology of the Universe

By

Sara Lykken

Advisers : Emily Hamilton and David Borthwick

An abstract of
A thesis submitted to the Faculty of Emory College of Arts and Sciences
of Emory University in partial fulfillment
of the requirements of the degree of
Bachelor of Sciences with Honors

Department of Mathematics and Computer Science

2010

Abstract

Harmonics Echoing Across Time and Space: A Summary of Research on the Topology of the Universe

By Sara Lykken

On June 30, 2001 NASA launched its Wilkinson Microwave Anisotropy Probe (WMAP) to study the Cosmic Microwave Background (CMB) radiation, radiation from the plasma that filled the universe until just 380,000 years after the Big Bang. The information collected by the WMAP satellite provides clues as to the universe's topology. Specifically, early WMAP data suggested the near disappearance of temperature fluctuations in the CMB radiation on large angular scales, going completely against what was predicted by an infinite Euclidean model for the universe. Researchers attempted to explain the missing large-scale fluctuations by suggesting the possibility of a small, finite-volume universe. Observations about the local geometry of our universe suggest a spherical, Euclidean or hyperbolic universe and, primarily for reasons of practicality, research has focused on spherical 3-manifolds. Comparing observed fluctuations in the CMB radiation to those predicted by various spherical spaces, some advocate the Poincaré dodecahedral space as a model for our universe. Recently, however, new data has been released that may weaken the case for the dodecahedral space. This paper seeks to explain and expand upon these topological investigations with the intention of making them accessible to a wider audience, in order to facilitate dialogue with specialists in other relevant areas.

Harmonics Echoing Across Time and Space:
A Summary of Research on the Topology of the Universe

By

Sara Lykken

Advisers : Emily Hamilton and David Borthwick

A thesis submitted to the Faculty of Emory College of Arts and Sciences
of Emory University in partial fulfillment
of the requirements of the degree of
Bachelor of Sciences with Honors

Department of Mathematics and Computer Science

2010

Contents

1	Introduction	1
2	The geometry of our universe	3
3	Constructing a model of the universe	11
4	Hearing the shape of the universe	20
5	A spherical universe?	27
6	Searching for a suppressed quadrupole	33
7	Do physical observations support the predictions of a dodecahedral model?	37
8	New evidence	40
9	Appendix A	43
10	Appendix B	45

List of Figures

1	An octagon in the hyperbolic plane	6
2	Straight lines in the hyperbolic disk model	7
3	Forming an octagon with 45° angles	7
4	Tiling the hyperbolic plane with octagons	8

		2
5	A piece of the hyperbolic plane	8
6	A flattened piece of the hyperbolic plane	9
7	Triangles in E^2, S^2 and H^2	10
8	A circle on a sphere's surface	17
9	The CMB power spectrum	22
10	Constructing a lens space	35
11	Seeing large-scale fluctuations in a finite-volume universe	44

List of Tables

1	Possibilities for m^{th} -degree monomials on the 3-sphere	24
2	Finite Symmetry Groups of S^2	29

1 Introduction

In its earliest stages, our universe was approximately one-millionth of its current size and so hot that electrons could not associate with nuclei. Photons were able to interact with these free electrons, creating a hot, glowing fog – known as plasma – that filled the universe. Approximately 380,000 years after the Big Bang, the continued expansion of the universe had finally allowed it to cool enough to permit the formation of atoms. The attachment of electrons to nuclei meant that there were no longer free-floating electrons for photons to interact with, thus permitting photons to begin traveling freely. The period after which photons began traveling undisturbed is known as *photon decoupling* and was the last stage in the formation of the Cosmic Microwave Background (CMB) radiation. When the cosmic microwave background first formed, the photons were approximately 3000 Kelvin, putting them at near infrared wavelength. Since then, the universe has expanded by a factor of approximately 1100, and the once visible radiation has stretched into microwaves with a wavelength of about a millimeter. These microwaves constitute the CMB radiation, and they fill the background of our universe.

The finite speed of light means that we see objects in space as they were in the past. We observe most stars as they were 10 to 100 years ago, and we see the spiral galaxy of Andromeda as it was 2.5 million years ago [2]. When we look far out into the distance, we see the Cosmic Microwave Background radiation as it was when the universe was only about three-thousandths of one percent of its current age, so the CMB radiation gives us a glimpse into the universe as it was during the final stages

of the big bang. Therefore, CMB radiation provides some of the most important information about the birth, expansion, geometry and topology of the universe.

On June 30, 2001 NASA launched the Wilkinson Microwave Anisotropy Probe (WMAP) to study this CMB radiation. Although the CMB radiation is exceptionally homogeneous, it is not perfectly so, demonstrating temperature fluctuations on the order of one part in 10^5 . These temperature fluctuations result from density fluctuations in the primordial plasma: photons coming from denser regions have to work harder against gravity and thus lose more of their energy and arrive cooler than the average photon. Conversely, photons coming from less dense regions lose less energy as they do not have to work as hard against gravity, so they arrive a little bit warmer than their counterparts coming from denser regions. Thus, the temperature fluctuations detected by the WMAP reflect density fluctuations in the radiation in the early universe.

Cosmologists expected to find density fluctuations on all scales, in accordance with the concordance model's prediction of an infinite and eternally expanding Euclidean universe. They were surprised to learn that, although the WMAP data confirms the existence of these fluctuations on small angular scales, the fluctuations essentially disappear for sections of the universe separated by more than about 60° . How can it be that the WMAP did not find the expected large-scale fluctuations? In his paper *The Poincare Dodecahedral Space and the Mystery of the Missing Fluctuations*, Jeffrey Weeks presents an overview of what these missing fluctuations might tell us about the shape of the universe [1]. This paper seeks to expand upon Weeks'

ideas, providing additional background and a more extensive discussion on the implications of these missing fluctuations, with the intention of making this topic more accessible to less specialized readers.

2 The geometry of our universe

We begin with a brief introduction to manifolds and, more specifically, spherical, Euclidean and hyperbolic spaces. For more information on these topics, see [3].

A *three-manifold* is a space in which every point is contained in a neighborhood homeomorphic to a subset of \mathbb{R}^3 , and these neighborhoods must fit together nicely to cover the space. This idea can perhaps be better understood through a lower-dimensional analogy. One can think of the pages of an atlas as neighborhoods making up the surface of a globe: each page of the atlas is flat and two-dimensional, and the pages can fit together nicely to cover all of the points on the surface of the three-dimensional globe. Similarly, on a small enough scale, a three-manifold looks like three-dimensional Euclidean space – that is, the “ordinary” 3-D space that we are used to – and these 3-dimensional sections fit together to cover the entire manifold. Our knowledge of the universe’s topology is extremely limited, so we use as a starting point the seemingly fair assumption that the local topology everywhere throughout the universe is like that of the space we live in on Earth. Therefore, because the space we occupy has the local topology of three-dimensional Euclidean space, it is generally assumed that the universe is a three-manifold. But *which* three-manifold do we live in?

Clues from our universe's local geometry can be used to rule out candidates in the search for the topology of the universe. Recall that the *topology* of a space refers to the properties of that space that are unaffected by continuous deformation – that is, bending, stretching, twisting, etc., but *not* tearing or gluing. A sphere and a cube are topologically equivalent surfaces since, given either a sphere or a cube made from Play-Doh, one could easily mold the dough to make the other surface without ripping or “gluing” the dough. A sphere is topologically different from a doughnut because a doughnut has a hole in it whereas a sphere does not, and neither of the surfaces can be deformed to look like the other without tearing or gluing. In contrast, a space's *geometry* refers to those properties that *are* affected by deformation – properties such as curvature, volume, distance and angle. These properties can help us determine the topology of the space since not every space can *admit*, or be given, every geometry.

The observable universe is believed to be both homogeneous (i.e. its local geometry is the same everywhere) and isotropic (its geometry is the same regardless of the angle of observation). Evidence such as the fact that the rate of expansion of the universe is the same in all directions and that CMB radiation is distributed in the same way in all directions to a precision of less than one part in 10^4 , suggests the isotropy of the observable universe. Of course, the fact that the *observable* universe is homogeneous and isotropic does not necessarily mean that the universe as a whole possesses these properties, but it does provide some support for the assumption of a homogeneous and isotropic universe and has led researchers to focus

on homogeneous, isotropic three-manifolds while trying to determine the topology of the universe.

The only locally homogeneous and isotropic spaces are those admitting a geometry of constant curvature – that is, spherical, Euclidean or hyperbolic geometry. Before going further, let's review some facts about these three geometries.

In order to illustrate a fundamental difference between the three geometries, we will begin by drawing a triangle on each of three different surfaces: a sphere S^2 , the standard Euclidean plane E^2 , and the hyperbolic plane H^2 . While the sphere and the infinite plane are familiar objects, the hyperbolic plane may not be. In the same way that the Euclidean plane E^2 can be tiled by an infinite collection of unit squares, one can think of constructing the hyperbolic plane by tessellating an infinite space with identical regular octagons. Of course, in the familiar Euclidean plane such a task would not be possible since eight octagons cannot fit around a central octagon without overlapping. However, if we shrink the angles in the octagons to 45° – and thus pass the octagons to a hyperbolic space – we *can* fit eight octagons around a central one (see Figure 1). But how do we shrink the angles of an octagon? To answer this question, we will use Henri Poincaré's famous model for the infinite hyperbolic plane (see Figure 4), in which H^2 is portrayed as an open unit disk whose boundary represents infinity. The Poincaré disk model has its own metric – distinct from the familiar Euclidean metric – for measuring distance, area and angles, although interestingly Euclidean and hyperbolic angles are equal. Because of this metric, hyperbolic straight lines are depicted in the model as arcs that are

orthogonal to the disk's boundary (Figure 2). The closer a hyperbolic straight line is to the disk's center, the less it appears to bend. If we place a small octagon in the center of the disk, its sides will be nearly straight and its angles close to 135° . Now we can stretch the octagon's vertices away from the center of the disk so that its angles are as small as we like. By continuity, we will be able to move the vertices just far enough from the center to form an octagon with angles of exactly 45° . We can then identify the octagon's sides as shown in Figure 3, thereby forming a group of isometries. Now, allowing this group to act on the octagon, we can tile the hyperbolic plane with an infinite number of copies of our octagon.

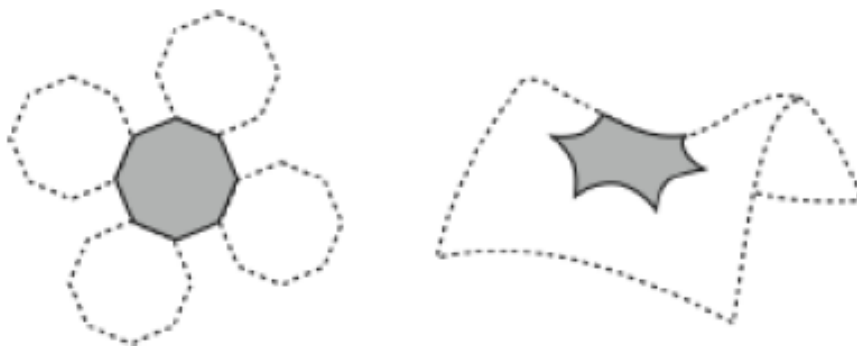


Figure 1: Although we cannot tessellate the Euclidean plane with flat octagons with angles of 135° , we can tessellate the hyperbolic plane with octagons cut from a saddle and with angles of 45° . Figure courtesy of Luminet. [4]

In many ways, we can think of the hyperbolic plane as opposite to the sphere, and this can help us visualize the hyperbolic plane. Locally a sphere seems bowed out, while the hyperbolic plane, in contrast, is locally saddle-shaped. If you took a piece of a sphere and tried to flatten it, the piece would have to split open in order to lay flat. If you flattened a piece of hyperbolic space, on the other hand,

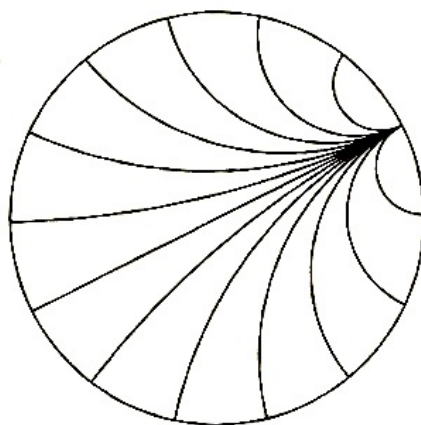


Figure 2: In the Poincaré disk model, hyperbolic straight lines are depicted as arcs orthogonal to the disk's boundary. Figure courtesy of Thurston [16].

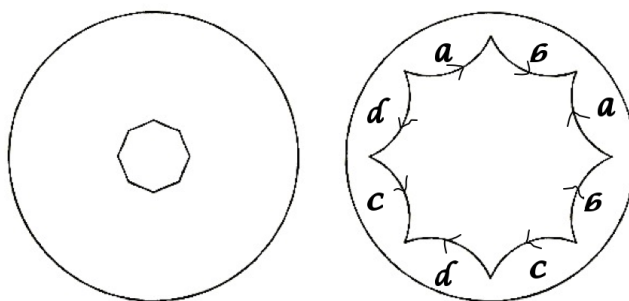


Figure 3: A small, nearly Euclidean octagon in the center of the circle (right) can be stretched into an octagon with 45° angles (left). We can then identify the sides of our octagon as shown.

the piece would wrinkle and fold over itself (see Figure 6). Such properties of the sphere and hyperbolic plane may cause one to wonder how, exactly, we will draw a triangle with “straight” edges on all of these surfaces. We answer this question by defining a “straight” edge in more general terms than one may be accustomed to. Each side of the triangle must be a *geodesic*, meaning that it must be the shortest path connecting the two vertices that serve as its endpoints. A geodesic is an intrinsically straight line in that a two-dimensional object living on the surface,

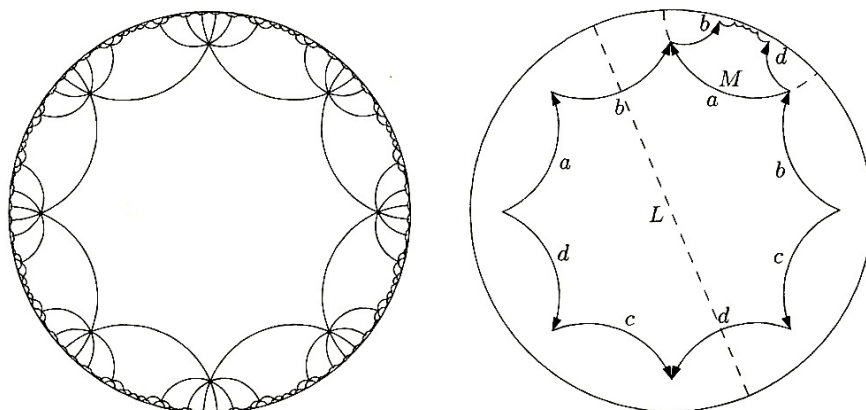


Figure 4: The Poincaré disk model portrays the infinite hyperbolic plane as a disk whose boundary represents infinity. Using this model, we see a tiling of the hyperbolic plane by octagons (right). Note that, although the copies of the octagon closer to the boundary of the disk appear smaller, this apparent change in size is due to the metric of the Poincaré disk model; the octagons are all identical copies that are hyperbolically isometric to one another. On the left, we see that the two copies of the octagon can be mapped onto each other by a reflection over the geodesic L , followed by a reflection over the geodesic M . Figure courtesy of Thurston [16].

with no knowledge of the outside three-dimensional world in which the surface is embedded, would not feel that it bent to the right or left.

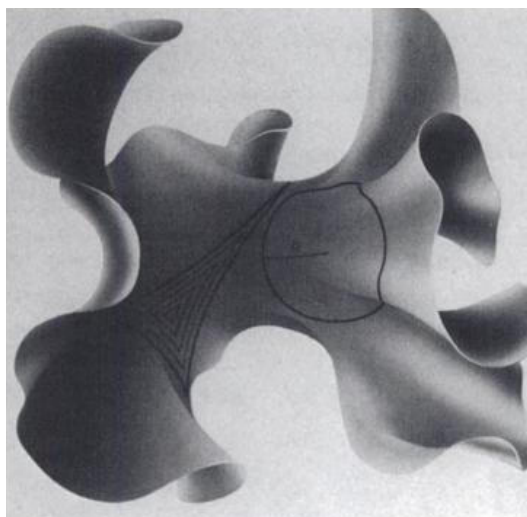


Figure 5: A piece of the hyperbolic plane. Note that H^2 is locally saddle-shaped. Figure courtesy of Weeks [3].

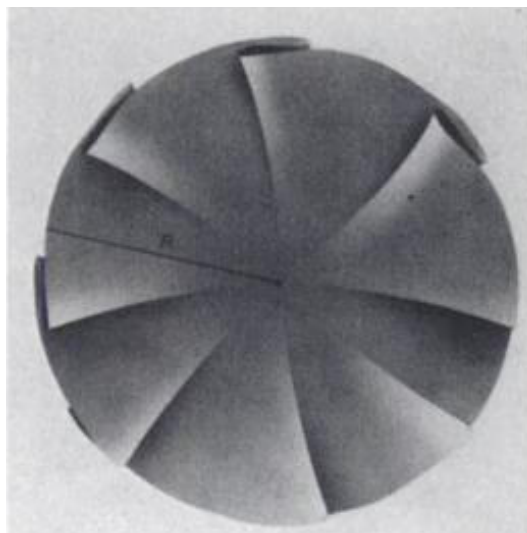


Figure 6: When flattened, a piece of the hyperbolic plane would wrinkle. Figure courtesy of Weeks [3].

We already know from basic principles of Euclidean geometry that the angles of a triangle drawn in the Euclidean plane E^2 will add up to 180° , or π radians. But what about the angles of a triangle drawn on the surface of a sphere or in the hyperbolic plane? It turns out that on S^2 the angles will add up to more than π , and on H^2 they will add up to less than π . Specifically, the sum of the angles of a spherical triangle is equal to π plus the area of the triangle, while in the hyperbolic plane the sum of a triangle's angles is equal to π minus the area of the triangle. This idea carries over to all polygons. For example, in the Euclidean plane, every hexagon has angles summing up to 120° . On the sphere, however, bigger hexagons have bigger angles and in the hyperbolic plane, bigger hexagons have smaller angles.

The geometry of a sphere is termed *spherical geometry* and is said to have constant curvature of $+1$; that of the Euclidean plane is called *Euclidean geometry* and is said to have zero curvature; and that of the hyperbolic plane is known as *hy-*

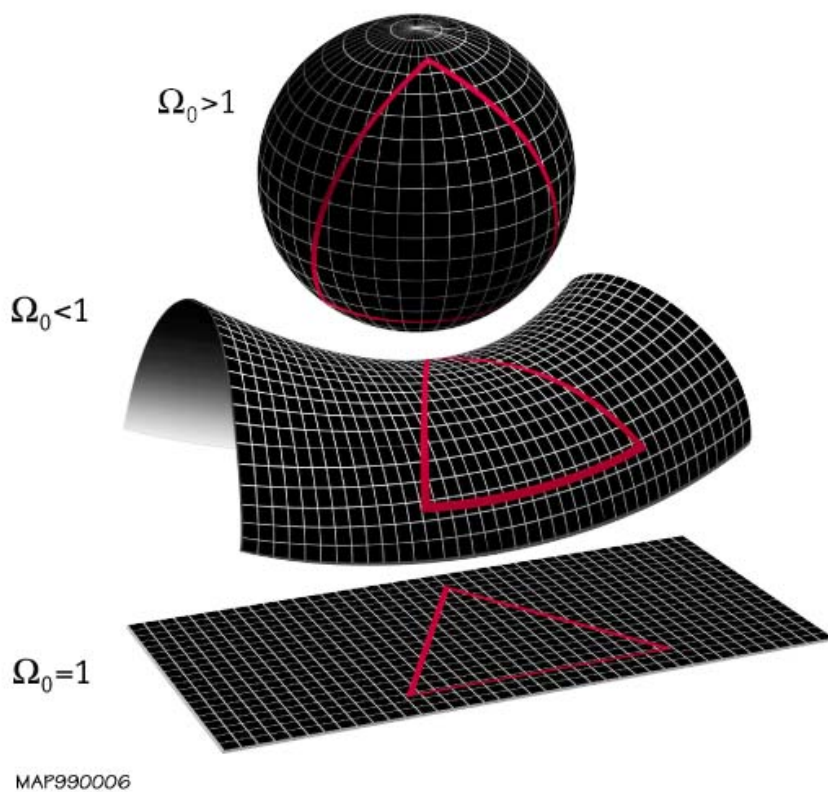


Figure 7: The angles of a triangle add to 180° in the Euclidean plane, more than 180° on a spherical surface, and less than 180° on a hyperbolic surface. Figure courtesy of NASA.

perbolic geometry and has constant curvature of -1. More specifically, given a line L and a point p not on L , a spherical geometry is one in which there is no line parallel to L and passing through p , Euclidean geometry is one in which there is exactly one such line, and hyperbolic geometry is one in which there are more than one such line. Of course S^2 , E^2 and H^2 are not the only manifolds admitting one of these geometries: in particular, their three-dimensional analogs S^3 , E^3 and H^3 admit a spherical, Euclidean and hyperbolic geometry, respectively. Our focus in this paper will be on 3-manifolds that admit one of these three geometries of constant curvature.

3 Constructing a model of the universe

The surprisingly low quadrupole value in the CMB power spectrum tells us that an unusually low number of large-scale fluctuations were observed in the background radiation. One explanation for this could be that we live in a small, finite-volume universe. Just as a vibrating piece of string with fixed endpoints cannot support a wavelength of oscillation longer than twice the length of the string, a small enough universe would have an upper limit on the length of waves it could support. Perhaps, then, the large-scale fluctuations were too large for our universe and therefore the WMAP observed very few fluctuations on this scale. (To understand how it would be possible to observe *any* large-scale fluctuations given such a small universe, see Appendix A.) We will use this possible explanation to help us narrow down our list of potential models for our universe and will consider only finite-volume manifolds.

By Hopf's Theorem, any finite-volume three-manifold with constant curvature will be a quotient X/Γ where the universal covering space $X = S^3, E^3$ or H^3 and where the holonomy group Γ is a subgroup of isometries that is properly discontinuous. Let's break this idea down a bit.

A *holonomy group* is a group of symmetries that is discrete and has no fixed points. Modding out by a symmetry, we preserve the metric and geometry of X . A trivial holonomy group signifies a simply connected space, while a nontrivial holonomy group implies a multiply connected space. We can think of a simply connected space as one in which any string made into a loop can be tightened into a small knot. On the other hand, in a multiply connected space, some loops will be wrapped around a hole and thus will not be able to be tightened into a knot: the loop will get stuck on the hole. A multiply connected space is the result of the identification of points within the space, so, in theory, a multiply connected universe could allow us to see multiple images of a single object, while a simply connected universe would not. The unit hypersphere S^3 is the only compact, homogeneous and isotropic three-manifold that is simply connected.

If the holonomy group is discrete and X/Γ has finite volume, there is a *fundamental domain* of the group that is a polyhedron with a finite number of faces [4]. Allowing the transformations in the holonomy group to act on each point in the fundamental domain tessellates a larger space, called the *universal covering space*, with copies of the fundamental domain polyhedron. Thus X/Γ is a space with the same local geometry as X , but in which each point is identified with other points

in X according to the symmetries of Γ .

During the earliest stages of the universe's evolution, electrons were not attached to individual nuclei and would interact with any radiation present. Eventually, however, the universe cooled down enough for electrons to begin joining with nuclei to form atoms. Because photons cannot interact freely with atoms, the attachment of all the free electrons to nuclei meant that each photon had a final interaction with an electron, after which the photon was able to travel freely. All this took place during a time when the universe was only about a thousandth of its current size, so the photons have been traveling for most of the life of the universe. Therefore, the photons received at any point x in the universe originated on the surface of an enormous sphere centered at x . This surface is called a *last scattering surface*. Note that, although every point in the universe has its own last scattering surface encompassing it, when we refer to *the* last scattering surface, we are referring to that of the Earth. The *horizon radius* is the radius of the last scattering surface, and the *horizon sphere*, or *observable universe*, is the Earth-centered sphere with radius equal to the horizon radius. It is within this horizon sphere that we perceive the primordial plasma.

In contrast to the observable universe lies the physical universe. We define the *injectivity radius* at a point x in our universe X/Γ as the radius of the largest ball, centered at x , such that no two elements of the ball are identified with one another. That is, if p maps X into X/Γ , then the injectivity radius at a point $x \in X/\Gamma$ is $injrad(x) = \sup\{\varepsilon > 0 : p \text{ is one-to-one on } B(x, \varepsilon)\}$. When we talk about *our*

injectivity radius, we are referring to the injectivity radius at the point y , where y represents the center of the Earth. So our injectivity radius is the radius of the smallest Earth-centered sphere that “reaches all the way around the universe and intersects itself”, and thus it represents a lower bound on the radius of the universe, starting from Earth.

We now have three possibilities: one, the universe could have infinite volume; two, the universe could have finite volume but our injectivity radius could be greater than (or equal to) our horizon radius; or three, the universe could have finite volume with the horizon radius exceeding our injectivity radius. Using observable data to distinguish between possibilities one and two would prove difficult, but if the horizon radius is greater than our injectivity radius, in theory we should be able to see multiple images of the same sources – for example, images of the same galaxy or the same distribution of the primordial plasma in various different parts of the sky.

In a Euclidean manifold, the injectivity radius at a point x is arbitrary in the sense that it is not a topological invariant, but depends on the isometry group Γ . To see this, suppose that $M_1 = E^3/\Gamma_1$ and let $\Gamma_2 = g\Gamma_1g^{-1}$, where $g : E^3 \rightarrow E^3$ is the Euclidean similarity taking x to cx . We can define a homeomorphism from M_1 to $M_2 = E^3/\Gamma_2$ by $[x] \mapsto [cx]$. Note that if the point $x \in M_1$ has injectivity radius ε , then the corresponding point cx in M_2 has injectivity radius $c\varepsilon$. Therefore, M_1 and M_2 are homeomorphic (i.e. they are topologically equivalent spaces), but they are not isometric (i.e. they are geometrically distinct spaces). The injectivity radius of a point in a Euclidean space depends on the metric and consequently is not well-

defined. Obviously, then, we cannot assume any logical relationship between the horizon radius and our injectivity radius in a Euclidean universe, and therefore it would be only with great luck that we would be able to detect a Euclidean topology E^3/Γ .

Fortunately, a hyperbolic universe would not present this problem since, by the Mostow Rigidity Theorem, any two finite-volume hyperbolic 3-manifolds that are homeomorphic are also isometric. Unfortunately, however, a compact hyperbolic topology may still be extremely difficult to detect. To see why, we must first distinguish between the previously defined horizon radius and what we will call the *geometer's horizon radius*. The previously defined horizon radius is already known to be approximately 46 billion light-years¹, but geometers are interested in knowing the horizon radius in radians, not light-years. Thus the geometer's horizon radius is the ratio of the horizon radius to the *curvature radius*, where the curvature radius is measured in light-years.

We already know that in Euclidean space, the circumference of a circle of radius r is $\ell = 2\pi r$. To find the circumference in spherical space, we can imagine drawing a circle on the surface of a sphere. Let the point a be the center of the circle, b be the center of the sphere, and c be any point on the circumference of the circle. Draw lines connecting point a to b , b to c and c to a , as shown, forming a right triangle. If

¹A 46 billion light-year horizon radius is made possible in a 13.7 billion-year-old universe by the universe's expansion. Because the universe is about 1100 times larger now than it was at the time of photon decoupling, the same space that the photons covered during their first year of uninhibited travel, for example, would now take approximately 1100 years to travel across. Thus the 46 billion light-year horizon radius reflects the fact that the universe was once considerably smaller and, if it would now take a photon one year to travel across a given space, it would have taken only a fraction of that time billions of years ago.

R is the radius of the sphere, then we have that $\sin \theta = \frac{s}{R}$ and therefore $s = R \sin \theta$.

Now the circumference of the circle is

$$\ell = 2\pi s = 2\pi R \sin \theta \quad (3.1)$$

Now, in order to relate r and θ , we note that the great circle on which the radius of our circle lies, will have circumference $2\pi R$ and correspond to an angle of 2π , while r corresponds to an angle of θ . This means that we can set up the ratio $\frac{\theta}{2\pi} = \frac{r}{2\pi R}$, and so $\theta = \frac{r}{R}$. Therefore, Equation (3.1) becomes

$$\ell = 2\pi R \sin \frac{r}{R}$$

(A similar argument works for hyperbolic space, in which $\ell = 2\pi R \sinh \frac{r}{R}$.) Thus, in theory we can determine our universe's curvature radius, R , experimentally by measuring values for ℓ and r and then plugging into this equation to solve for R . Note that in Euclidean space, $R \rightarrow \infty$ and thus $\ell = 2\pi R \sin \theta = 2\pi R(\theta - \frac{1}{6}\theta^3 + \dots) = 2\pi r(1 - \frac{r^2}{R^2} + \dots)$ approaches $2\pi r(1 + 0) = 2\pi r$, which is the equation we would expect in Euclidean space.

Definition 3.2. The *Normalized Density Parameter* Ω is the ratio of the actual mass-energy density of space to the critical value $\frac{3H^2}{8\pi G}$ required by a Euclidean space, where H is the Hubble constant and G is the gravitational constant .

Einstein's field equations in general relativity relate curvature to the normalized density parameter Ω , telling us that the curvature of a space is completely

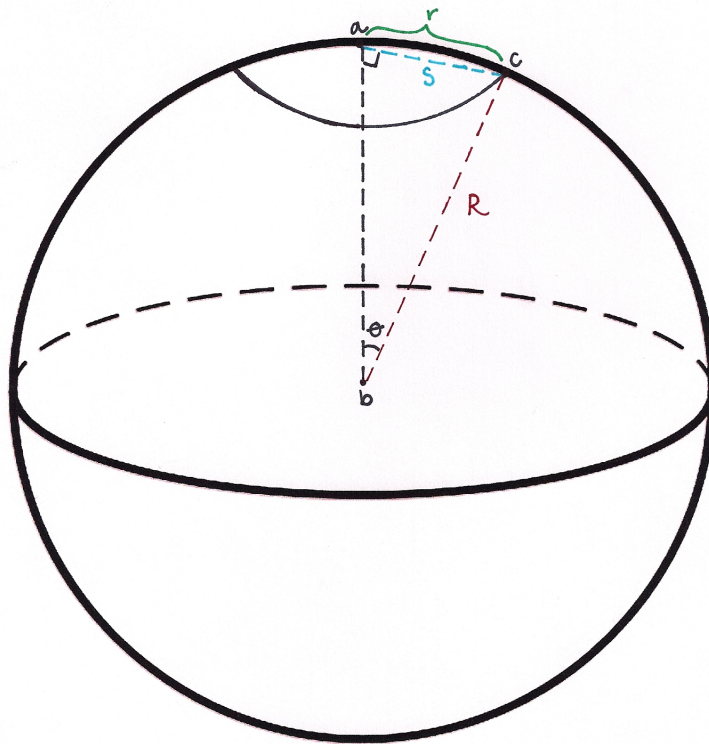


Figure 8: A circle on the surface of a sphere will have circumference $\ell = 2\pi R \sin \frac{r}{R}$.

determined by the matter and energy within that space². $\Omega > 1$ implies positive curvature, $\Omega = 1$ zero curvature, and $\Omega < 1$ negative curvature. Recall that S^3 has curvature equal to +1, H^3 has curvature of -1 and E^3 has zero curvature. To achieve other values of curvature, we can simply rescale the space: if we scale by λ , the curvature of the space will be multiplied by a factor of $1/\lambda^2$. Therefore, we can say that $\Omega > 1$ indicates spherical geometry, $\Omega = 1$ Euclidean geometry, and $\Omega < 1$ hyperbolic geometry. Thus the curvature radius, and consequently the geometer's horizon radius, depends on the value of Ω .

An observer at a point x could, in theory, detect the universe's topology if the geometer's horizon radius exceeds the injectivity radius at x , $injrad(x)$. In a 3-torus and in numerous spherical spaces, the value of $injrad(x)$ is constant for all x in the space, meaning that if the space's topology is theoretically detectable by an observer at point y in the space, it is also theoretically detectable by an observer at any other point in the space. The same does not hold for hyperbolic topologies. Because the injectivity radius at a point x in a hyperbolic space does not necessarily equal the injectivity radius at a different point y in that space, it is possible that the hyperbolic topology could be detectable by an observer at x by not by one at y if $injrad(x) < injrad(y)$. By creating "injectivity profiles" – that is, histograms displaying the percentage of a manifold's volume with a given injectivity radius

²In a general space, the value of R could vary from point to point, but we are only considering 3-manifolds of constant curvature, so R will be roughly the same everywhere. This may seem strange given Einstein's equation and the fact that some parts of space contain more mass than others (e.g. the area around a planet in contrast to an area of space containing no planets or stars). To reconcile the seeming discrepancy, it is important to keep in mind that *on average* the universe is thought to be homogeneous, so *on average* mass should be distributed evenly throughout and thus, by Einstein's equation, *on average* the curvature of space will be constant.

– for the first ten low-volume hyperbolic manifolds in the Hodgson-Weeks census, Weeks was able to calculate the probability that a randomly-placed observer in each of these manifolds would be located at a point x where $injrads(x)$ is greater than a given horizon radius [5]. Averaging these probabilities over the ten manifolds, one can see that the chances of us being able to detect a hyperbolic topology are relatively low.

If $\Omega = 0.98$, the curvature radius is approximately 98 billion light-years, so the geometer’s horizon radius is $46/98 \approx 0.47$, and a random observer in one of the ten smallest hyperbolic topologies would have a 50% chance of being in a location where her horizon radius is larger than the injectivity radius. If $\Omega = 0.99$, the curvature radius is about 139 billion light-years, so the geometer’s horizon radius decreases to $46/139 \approx 0.33$, and the random observer’s chances of being in a spot where her horizon radius exceeds the injectivity radius, go down to about 10%. As Ω goes to 1, her chances approach zero. When Weeks’ article [1] was originally published, data collected by the WMAP satellite indicated that $\Omega = 1.02 \pm 0.02$ at the 1σ level. Given this, in a hyperbolic universe Ω is likely to be close to 1, meaning that our chances of detecting a hyperbolic topology do not look good. Furthermore, the volume of the quotient H^3/Γ increases as the complexity of Γ does, so the fact that the injectivity radius is usually larger than the horizon radius in even these ten smallest hyperbolic manifolds paints an even bleaker picture for those hoping to detect a hyperbolic universe.

A spherical universe S^3/Γ may prove much easier to detect. Here the radius

of curvature is just the radius of the hypersphere S^3 , and when $\Omega = 1.02$, this translates to a geometer's horizon radius of 0.47 radians. Fortunately, this horizon radius is large enough to allow us to detect the topology S^3/Γ for most of the simplest, most natural spherical groups Γ . Furthermore, unlike hyperbolic groups, as spherical groups Γ become more complicated, their quotient spaces S^3/Γ get smaller. So for more complicated groups Γ , the topology is even easier to detect. The spherical universe's greater likelihood of being detectable, coupled with the WMAP data's suggestion that $\Omega = 1.02$, has led many researchers to focus their studies on spherical manifolds.

4 Hearing the shape of the universe

In the very early universe, before the differentiation of matter from light, particles began to vibrate under the pressure of two opposing forces: that of gravity and of radiation. When the CMB formed and photons were at last able to travel freely, they retained an indication of this vibration in the form of temperature fluctuations representing the density fluctuations in the primordial plasma. Just as a musical tone can be decomposed into fundamental harmonics, the density distribution of the primordial plasma can be decomposed into harmonics of 3-dimensional space. The harmonics of a 3-dimensional space are simply the eigenmodes of the Laplace operator, but we can understand them as the vibrational modes of space, comparable to the vibrational modes – the harmonics – of a 2-dimensional drumhead. The way a drum sounds – determined by the relative strengths of the drum's harmonics –

depends on the way in which the drum was initially struck, the drum's material composition, the curvature of its surface and the shape of its boundary. In the same way, the relative strengths of the vibrational modes of space provide information about initial fluctuations in the universe, the matter and energy it contains, spatial curvature, and the topology of the universe.

In music, the fundamental harmonic determines pitch, and the relative amplitude of each harmonic determines the timbre; thus, an instrument's harmonics characterize its sound. In analogy to the way that pressure and density fluctuations inside a clarinet provide information about the size and shape of the clarinet, pressure and density fluctuations in the primordial plasma can tell us much about the size and shape of our universe. Looking deep into space at our horizon, we can see the density fluctuations in the CMB radiation – more specifically, we see the intersection of the 3-dimensional eigenmodes with our 2-dimensional horizon sphere, and the strengths of these observed modes are the *CMB power spectrum*. This spectrum shows the temperature fluctuations on the last scattering surface, as dependent on the angle of view. For example, the first observable harmonic, the quadrupole (with wave number $\ell = 2$), corresponds to an angle of observation of 90° .

We look for evidence of the shape of our universe by comparing the observed temperature fluctuations in the CMB with those that would be expected given a certain topology. One can calculate the eigenmodes of the Laplacian for a given topological space and then, using a set of initial conditions, simulate the evolution of these harmonics through time to the present day in order to generate a predicted

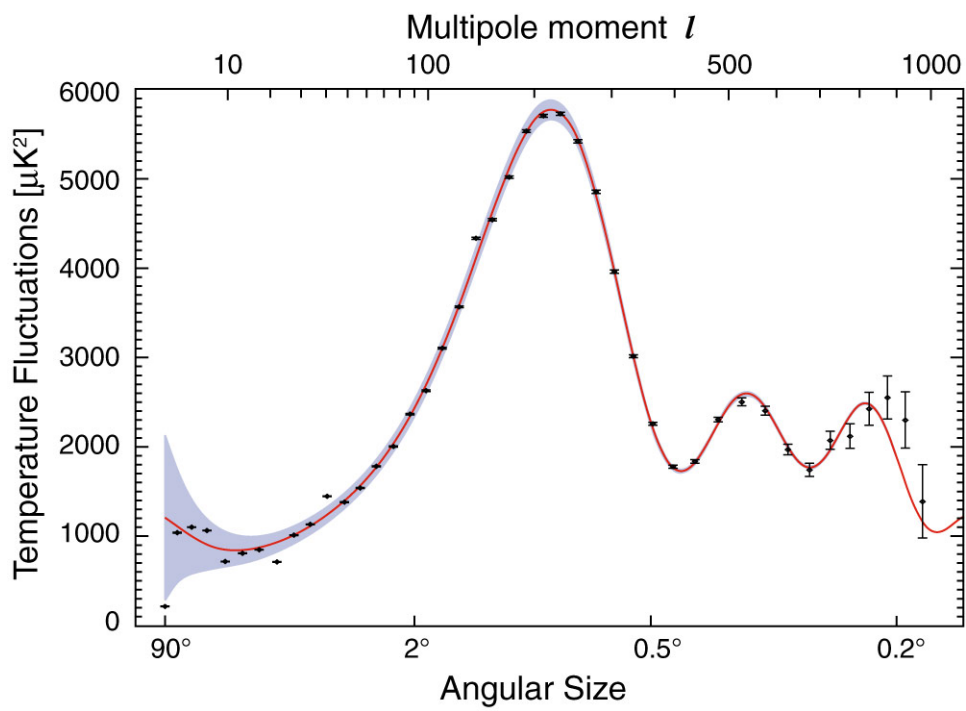


Figure 9: The density distribution of the primordial plasma can be decomposed into harmonics of 3-dimensional space, in the very same way that a musical tone can be decomposed into fundamental harmonics. Figure courtesy of the NASA/WMAP Science Team.

map of the CMB. The calculation of how a 3-manifold's eigenmodes restrict to our 2-dimensional horizon sphere are relatively simple, allowing for the direct comparison of predicted to observed harmonics. The primary complication, then, is calculating the eigenmodes for a candidate topological space.

If our universe X/Γ (where $X = S^3, E^3$ or H^3) is multiply connected, its eigenmodes lift in the obvious way to Γ -periodic modes of its simply connected universal cover X . Additionally, if $p : X \rightarrow X/\Gamma$ is a covering map, then each Γ -periodic mode λ will project down to an eigenmode of X/Γ , namely $p(\lambda)$. Therefore, we can easily go back and forth between the eigenmodes of X/Γ and the Γ -periodic eigenmodes of X , so for ease of calculation we express the vibrational modes as Γ -periodic modes of X , even though conceptually we think of them as the eigenmodes of X/Γ .

We will focus on the eigenmodes of spherical space S^3 , which are regular and much easier to predict than those of hyperbolic space H^3 . Let's start off by examining the eigenmodes, or harmonics, of the circle S^1 . The harmonics of a circle are usually written as the set $\{\{\cos \theta, \sin \theta\}, \{\cos 2\theta, \sin 2\theta\}, \dots\}$. However, consider what happens if we embed S^1 in the xy -plane as the set $\{(x, y) \in \mathbb{R}^2 : x^2 + y^2 = 1\}$. Now, using trigonometric identities, we see that the transcendental functions $\cos \theta$ and $\sin \theta$ are equivalent to the linear functions x and y , respectively; $\cos 2\theta$ and $\sin 2\theta$ are equivalent to the quadratic polynomials $x^2 + y^2$ and $2xy$, respectively, etc. The general transcendental functions $\cos n\theta$ and $\sin n\theta$ are equivalent to n^{th} -degree harmonic polynomials in x and y .

Similarly, the eigenmodes of S^2 are the homogeneous harmonic polynomials in

x, y , and z , and those of the hypersphere S^3 are the homogeneous harmonic polynomials in x, y, z , and w . (Recall that a *homogeneous polynomial* is one in which all monomials with nonzero coefficients have the same total degree.)

Perhaps not so obviously analogous is the number of eigenmodes of the three spaces. On the circle S^1 , the space of the homogeneous harmonic polynomials has dimension 2, regardless of the degree of the polynomials. On S^2 , in contrast, the dimension of space of the n^{th} degree harmonic polynomials does depend on the degree, the dimension being $2n + 1$. Most relevantly to our discussion, the space of an m^{th} degree harmonic polynomial on S^3 has dimension $(m + 1)^2$. To see this, note that for any m^{th} degree monomial $x^a y^b z^c w^d$, the exponents are restricted by the equation $a + b + c + d = m$. Therefore, once values have been chosen for a and b , c can be at most $m - a - b$, and the value of d is completely determined by those of a, b and c using the equation $d = m - a - b - c$. Given this, the possibilities for m^{th} degree monomials on the 3-sphere are as follows:

Table 1: Possibilities for m^{th} -degree monomials on the 3-sphere

Degree of x	Degree of y	Number of Possibilities
0	0	$k + 1$
0	1	k
0	2	$k - 1$
...
0	k	1
1	0	k
1	1	$k - 1$
...
1	$k - 1$	1
...
k	0	1

So the total number of possibilities is given by the sum

$$\begin{aligned} & [(m+1)+m+(m-1)+\dots+1]+[m+(m-1)+\dots+1]+[(m-1)+(m-2)+\dots+1]+\dots+1 \\ & = (m+1) + 2m + 3(m-1) + \dots + m * 2 + (m+1) * 1 \end{aligned}$$

Note that any homogeneous polynomial of degree m is a linear combination of monomials of degree m and all the monomials of degree m with a coefficient of 1 are linearly independent, so this sum represents the dimension of the space of *all* homogeneous polynomials of degree m in x, y, z , and w . Now to find the dimension of the space of only the harmonic homogeneous polynomials of degree m , we must recall that, by definition, a polynomial $p(x_1, x_2, \dots, x_n)$ is *harmonic* if and only if it satisfies Laplace's equation

$$\nabla^2 p \equiv \frac{\partial^2 p}{\partial x_1^2} + \frac{\partial^2 p}{\partial x_2^2} + \dots + \frac{\partial^2 p}{\partial x_n^2} = 0 \quad (4.1)$$

Let A be the space of all homogeneous polynomials of degree m and B the space of all homogeneous polynomials of degree $m - 2$. Note that, if p is a homogeneous polynomial of degree $m \geq 2$, then the Laplacian acting on p will produce a homogeneous polynomial of degree $m - 2$, since each term will either be zero or nonzero of degree $m - 2$. Consequently, we can define a map $f : A \rightarrow B$ that takes $p \mapsto \nabla^2 p$. It turns out that this map is a surjective homomorphism, meaning that every homogeneous polynomial of degree $m - 2$ is the Laplacian of an m^{th} degree homogeneous polynomial [6].

Therefore, the dimension of the space of homogeneous harmonic polynomials of degree m on the 3-sphere will be equal to the dimension of the space of homogeneous polynomials of degree m minus the dimension of the space of homogeneous polynomials of degree $m - 2$:

$$\begin{aligned}
& (m+1) + 2m + 3(m-1) + \dots + (m-1) * 3 + m * 2 + (m+1) * 1 - [(m-1) + 2(m-2) + \dots + (m-2) * 2 + (m-1) * 1] \\
&= (m+1) + 2m + 2(m-1) + 2(m-2) + \dots + 2 * 2 + 2 * 1 \\
&= (m+1) + 2[m + (m-1) + (m-2) + \dots + 2 + 1] \\
&= (m+1) + 2[(m)(m+1)/2] \\
&= (m+1) + m(m+1) \\
&= m+1 + m^2 + m \\
&= m^2 + 2m + 1 \\
&= (m+1)^2
\end{aligned}$$

In order to simulate the physics of a multiply connected spherical universe S^3/Γ , cosmologists use the Γ -periodic modes of S^3 , as discussed previously. For every degree m , these Γ -periodic modes form a subspace of the $(m+1)^2$ -dimensional space of m^{th} -degree polynomials on S^3 . Although in theory finding an orthonormal basis for these subspaces should be simple, in reality the linear algebra becomes extremely complicated as the value of m gets larger. Additionally, many of the computations that can be done in a more reasonable amount of time end up being unfit for use due to accumulated rounding errors.

The difficulty of computing the eigenmodes has been a serious hindrance to cosmologists trying to understand and to model the physics of multiconnected spaces. Fortunately, in 2005 Jesper Gundermann published calculations of the Γ -periodic eigenmodes of S^3 for the binary polyhedral spaces S^3/T^* , S^3/O^* , and S^3/I^* , up to $k = 100$ [7]. Then, using symmetry properties of these eigenmodes, he derived estimates for the ℓ -terms of the CMB power spectra and their variances up to $\ell = 15$, when previously the CMB power spectra for these spaces were only known up to $\ell = 4$. The results of Gundermann's simulation of the CMB in the Poincaré dodecahedral space has interesting implications for the possibility of this space as a candidate for the shape of the universe, and shall be discussed later.

5 A spherical universe?

(This section assumes a basic understanding of abstract algebra. For relevant algebra theorems, please see the appendix. Proofs of these theorems can be found in [8].)

Data collected by the WMAP satellite favors a spherical universe and spherical spaces certainly seem easier to work with than hyperbolic ones, so it would make sense to test for the possibility of the universe being a spherical 3-manifold. Fortunately, all the 3-dimensional spherical spaces have already been classified (see [9]), so in theory we should be able to calculate the eigenmodes of – and simulate a power spectrum for – all spherical 3-manifolds in order to test whether any of their eigenmodes match up with physical observations. In order to understand how the spherical spaces have been classified, we must first review the quaternions, \mathbb{H} . The

quaternions provide a non-commutative algebraic structure on \mathbb{R}^4 and are spanned by the set $\{1, i, j, k\}$, where $i^2 = j^2 = k^2 = -1$, $ij = k$, $jk = i$, and $ki = j$. Just as S^1 has a natural multiplicative group structure as the set $\{x \in \mathbb{C} : |x| = 1\}$, S^3 has a natural multiplicative group structure as the set of unit length quaternions.

Now let $q \in \mathbb{H}$, and consider the effect of q acting on an element $x \in \mathbb{H}$ by conjugation. Note that for all $q \in \mathbb{H}$, the point $1 \in S^3$ will be fixed by conjugation by q since $q1 = 1q$ and thus, multiplying both sides by q^{-1} on the left, $q1q^{-1} = 1$. Therefore, we can think of conjugation by $q \in S^3$ as a rotation of the equatorial 2-sphere – that is, the intersection of S^3 with the span of the set of purely imaginary quaternions, $\{i, j, k\}$.

Recall that $SO(3)$ is the group of proper (i.e. length- and orientation-preserving) rotations of \mathbb{R}^3 . Then if conjugation by q is a rotation of the equatorial 2-sphere, each $q \in S^3$ defines an element $p_q \in SO(3)$, where p_q is the isometry sending $x \in \mathbb{H}$ to qxq^{-1} . Now consider the map $p : S^3 \rightarrow SO(3)$ defined by $p(q) = p_q$. This map is a homomorphism since

$$\begin{aligned} p(qr)(x) &= p_{qr}(x) \\ &= qr x (qr)^{-1} \\ &= qr x r^{-1} q^{-1} \\ &= p_q(p_r(x)) \end{aligned}$$

and thus $p(qr) = p(q)p(r)$ under the operation of function composition. We will

use this homomorphism to classify the subgroups of S^3 , but first we need a full classification of the finite subgroups of $SO(3)$.

Fortunately, the finite subgroups of $SO(3)$ are just the finite symmetry groups of S^2 . These groups are well-known and are listed in Table 2.

Table 2: Finite Symmetry Groups of S^2

Group	Order	Description
Cyclic groups Z_n	n	Generated by rotations of $\frac{2\pi}{n}$ radians about some axis
Dihedral groups D_m	$2m$	Symmetry group of the regular n-gon
Tetrahedral group T	12	Symmetry group of the regular tetrahedron
Octahedral group O	24	Symmetry group of the regular octahedron
Icosahedral group I	60	Symmetry group of the regular icosahedron

Returning now to the homomorphism p , we see that the kernel is

$$\begin{aligned}
 Ker(p) &= \{q \in S^3 : p_q(x) = x, \forall x \in S^3\} \\
 &= \{q \in S^3 : qxq^{-1} = x, \forall x \in S^3\} \\
 &= \{q \in S^3 : qx = xq, \forall x \in S^3\}
 \end{aligned}$$

But multiplication in \mathbb{H} is noncommutative and, in fact, if $a, b \in \mathbb{H}$ are nonreal, then $ab = ba \iff$ their imaginary parts are parallel. Therefore, we have that

$$Ker(p) = \{\pm 1\}$$

and thus p is a two-to-one mapping from S^3 into $SO(3)$. Let Γ be a finite subgroup of S^3 . Obviously $1 \in \Gamma$ since, by definition, groups contain an identity element, so we will now consider the cases where Γ does or does not contain -1 .

Case 1 ($-1 \notin \Gamma$): In this case, $Ker(p|_{\Gamma}) = \{1\}$ and thus $p|_{\Gamma}$ is a one-to-one mapping into $SO(3)$. Because p is a homomorphism and Γ a finite subgroup, we know that its image is a finite subgroup of $SO(3)$ by the properties of homomorphisms. Therefore, by the First Isomorphism Theorem, Γ must be isomorphic to one of the above listed finite symmetry groups of S^2 . In fact, we may narrow down the list of possibilities for Γ even further by noting that, since -1 is the only element of S^3 of order 2, Γ contains no elements of order 2. Cauchy's Theorem tells us that every finite group of even order has an element of order 2, and thus eliminates as possibilities all finite symmetry groups of S^2 except for the cyclic groups of odd order. At the same time, Lagrange's Theorem guarantees that no cyclic group of odd order will have an element of order 2, leaving all cyclic groups of odd order as possibilities.

We can see that for every odd integer n , there is, in fact, a cyclic subgroup of S^3 of order n that maps isomorphically into $SO(3)$ as follows: let n be odd, let $H_n \subset S^3$ be the multiplicative group of order n generated by the unit-length quaternion $\cos(\frac{2\pi}{n})\mathbf{1} + \sin(\frac{2\pi}{n})\mathbf{i}$, and let $\phi : H_n \rightarrow SO(3)$ be the restriction of p to H_n - that is, $\phi(q) = p_q$. Suppose, by way of contradiction, that $-1 \in H_n$. Then $\frac{2\pi k}{n} = \pi$ for some $k \in \{1, 2, \dots, n\} \Leftrightarrow 2k = n \Leftrightarrow n$ is even. $\rightarrow\leftarrow$ But this contradicts the fact that n is odd. We conclude that $-1 \notin H_n$ and thus that $Ker\phi = \{1\}$.

Consequently, by the properties of homomorphisms, ϕ is a one-to-one mapping from H_n into $SO(3)$. Then $|H_n| = |\phi(H_n)| = n$ and so $\phi(H_n)$ must be isomorphic to \mathbb{Z}_n since, for any odd value of n , \mathbb{Z}_n will be the only finite subgroup of $SO(3)$ of order n . Therefore, by the First Isomorphism Theorem, H_n is isomorphic to \mathbb{Z}_n . \square

Case 2 ($-1 \in \Gamma$): In this case, $\text{Ker}(p|_{\Gamma}) = \{1, -1\}$ and thus $p|_{\Gamma}$ is a two-to-one mapping into $SO(3)$. Therefore, Γ is a two-fold covering of one of the finite symmetry groups of S^2 . On the other hand, each of these symmetry groups lifts to a subgroup of S^3 . A binary polyhedral group is defined as the two-fold cover of a finite symmetry group $G \subset S^2$, constructed by simply taking the pre-image $p^{-1}(G)$. For example, if G is a cyclic group of order n , then $p^{-1}(G)$ is called the binary cyclic group of order $2n$; if G is the tetrahedral group (order 12), then $p^{-1}(G)$ is called the binary tetrahedral group (order 24), etc. The *binary cyclic group* of the n -gon is simply the cyclic group of order $2n$, so every cyclic group of even order is a binary cyclic group. Note that, in contrast, the dihedral, tetrahedral, octahedral and icosahedral groups are not subgroups of S^3 ; only their binary covers are.

Thus, by Cases 1 and 2, we have the complete classification of finite subgroups of S^3 :

- The cyclic groups \mathbb{Z}_n , of order n
- The binary dihedral groups D_n^* , of order $4n$, $n \geq 2$ (D_1 is isomorphic to \mathbb{Z}_4)
- The binary tetrahedral group T^* , of order 24
- The binary octahedral group O^* , of order 48, and
- The binary icosahedral group I^* , of order 120

To better understand how the subgroups of S^3 act on S^3 to form spherical 3-manifolds, we will first begin with a definition.

Definition 5.1. A *clifford translation* g of a metric space M is an isometry that translates all points to the same distance. That is, $\forall x, y \in M, d(x, g(x)) = d(y, g(y))$.

A *single-action manifold* S^3/Γ is one in which the elements of Γ act as right-handed Clifford translations, where Γ is a subgroup of S^3 . Here a right-handed Clifford translation corresponds to left multiplication by a unit-length quaternion q and acts as a right-handed corkscrew rotation of S^3 . A left-handed Clifford translation $x \mapsto xq$ acts as a left-handed corkscrew rotation of S^3 , causing S^3/Γ to be the mirror image of what it would be if Γ acted as a right-handed Clifford translation.

We can see why right multiplication – as opposed to left multiplication – reverses the direction of the corkscrew motion, through the following observation: notice

$$\begin{aligned} & \text{that } (\cos \theta \mathbf{1} + \sin \theta \mathbf{i})(a \mathbf{1} + b \mathbf{i} + c \mathbf{j} + d \mathbf{k}) \\ &= (a \cos \theta \mathbf{1} - \sin \theta \mathbf{i} \cdot (b \mathbf{i} + c \mathbf{j} + d \mathbf{k})) \mathbf{i} + \cos \theta (b \mathbf{i} + c \mathbf{j} + d \mathbf{k}) + a \sin \theta \mathbf{i} + (\sin \theta \mathbf{i}) \times (b \mathbf{i} + c \mathbf{j} + d \mathbf{k}) \\ &= (a \cos \theta + b \sin \theta) \mathbf{1} + (b \cos \theta + a \sin \theta) \mathbf{i} + (c \cos \theta - d \sin \theta) \mathbf{j} + (d \cos \theta + c \sin \theta) \mathbf{k}, \\ & \text{whereas } (a \mathbf{1} + b \mathbf{i} + c \mathbf{j} + d \mathbf{k})(\cos \theta \mathbf{1} + \sin \theta \mathbf{i}) \\ &= (a \cos \theta \mathbf{1} - (b \mathbf{i} + c \mathbf{j} + d \mathbf{k}) \cdot \sin \theta \mathbf{i}) \mathbf{i} + a \sin \theta \mathbf{i} + \cos \theta (b \mathbf{i} + c \mathbf{j} + d \mathbf{k}) + (b \mathbf{i} + c \mathbf{j} + d \mathbf{k}) \times (\sin \theta \mathbf{i}) \\ &= (a \cos \theta + b \sin \theta) \mathbf{1} + (b \cos \theta + a \sin \theta) \mathbf{i} + (c \cos \theta + d \sin \theta) \mathbf{j} + (d \cos \theta - c \sin \theta) \mathbf{k}. \end{aligned}$$

A *double-action manifold* is a quotient space in which two subgroups, Γ and Γ' of S^3 act simultaneously on S^3 as right- and left-handed Clifford translations, and each element in Γ occurs with each element of Γ' . A *linked action manifold* is like a double-action manifold, except that each element in Γ occurs with only

some elements of Γ' . All spherical 3-manifolds have been shown to belong to one of these three categories – single, double or linked action manifolds – so with the classification of finite subgroups of S^3 we obtain a complete classification of spherical 3-manifolds [9].

Cosmologists are currently focusing mainly on single-action manifolds for two main reasons: first, double and linked action spaces frequently require unrealistically complicated groups Γ ; and second, double-action manifolds are globally inhomogeneous, i.e. their geometries look different depending on the observer's location within the space. A single action space, however, is globally homogeneous, so its geometry – and thus the expected CMB power spectrum – look the same to every observer, regardless of her location in space. Clearly, then, single action spaces are much easier to work with since they assure that data collected on the CMB power spectrum from one observation point will be consistent with that collected from every other observation point.

6 Searching for a suppressed quadrupole

The $\ell = 0$ constant term tells us the average CMB temperature. The value of the $\ell = 1$ linear term from the WMAP data, generally called the dipole, reflects the dipole induced by the movement of the solar system relative to the CMB. The dipole induced by this relative movement is far stronger than the dipole in the CMB and thus overwhelms it. The removal of these two terms leaves the harmonics representing the intrinsic temperature fluctuations in the CMB radiation. At small

angular scales (large ℓ values), the WMAP data seems to coincide nicely with the infinite flat space model. At large angular scales (small ℓ values), however, it tells a different story. The $\ell = 2$ quadratic term, often called the quadrupole, had a measured value seven times weaker than what would be predicted by a flat, infinite universe model. The probability of such a great difference occurring by chance is only 0.2%. The $\ell = 3$ cubic term, called the octopole, was also found to be a fair amount weaker than expected, although the difference between its measured and expected values fell within the range of acceptable error. Of course, the differences could be due to chance, but when taken together, the facts that both the $\ell = 2$ and $\ell = 3$ terms were low and that the probability of such a great difference in the $\ell = 2$ term is so small, merit an investigation.

Mathematicians have studied various multiply connected topologies, looking to see how they affect large scale fluctuations. Results have shown that spaces in which not all dimensions are of similar magnitude are highly inconsistent with the WMAP data, in that they actually elevate the quadrupole instead of suppressing it. For example, among the Euclidean spaces, mathematicians have studied the rectangular oblate and prolate 3-tori, which are made by identifying opposite sides of rectangles. While these spaces do indeed suppress the low- ℓ terms, they lower the high- ℓ terms even more, thereby causing the quadrupole to be elevated in comparison. Similar conclusions were made regarding spherical spaces. A *lens space* $L(p, q)$ is the quotient S^3/\mathbb{Z}_p , made by identifying the lower and upper surfaces of a lens-shaped solid with a rotation of $2\pi q/p$, where $p, q \in \mathbb{Z}^+$, $p > q$, and p and q are relatively prime

(see Figure 10). Clearly not all dimensions of a lens space are of similar magnitude, and, in fact, it behaves in a manner somewhat similar to that of a rectangular 3-torus that is narrow in one direction and wide in the other two. Again, just as the oblate and prolate 3-tori, the lens spaces lowered the high- ℓ terms more than the low ones and thus effectively elevated the quadrupole.

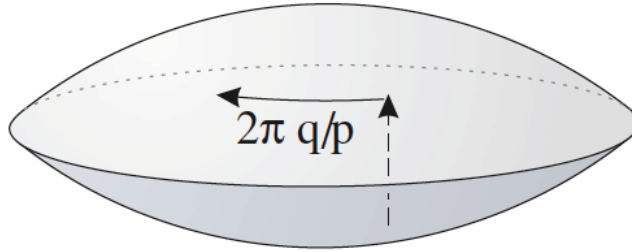


Figure 10: Constructing a lens space $L(p,q)$. Picture courtesy of Gausmann *et al* [9]

From this, mathematicians have concluded that only a “well-proportioned space” that is of similar magnitude in every dimension, can produce the desired low $\ell = 2$ term. Among the Euclidean topologies, they have examined the flat 3-tori and found that, although a small cubic 3-torus – made by identifying opposite sides of a cube – can lower the quadrupole, it also lowers the $\ell = 3, 4,$ and 5 terms. Obviously then, since the WMAP data show an only somewhat low octopole and normal $\ell = 4$ and 5 terms, a cubic 3-torus is not consistent with observations.

All of these results, together with the fact that WMAP estimates for Ω suggest a spherical universe, have caused researchers to look into the binary polyhedral spaces S^3/T^* , S^3/O^* , and S^3/I^* , as these spherical spaces have the nicely proportioned fundamental domains of a regular octahedron (a polyhedron with 8 triangular faces),

a truncated cube (with 6 octagonal and 8 triangular faces) and a regular dodecahedron (with 12 pentagonal faces), respectively. Conveniently, a circle inscribed in a regular dodecahedron has radius $\pi/10 \approx 0.31$. If we take Ω to be 1.02, then the geometer's horizon radius will be $0.47 > 0.31$ and thus, in theory, if the universe is in the shape of S^3/I^* , we should be able to see multiple images of the same source and detect the universe's topology. For this reason, mathematicians have focused on S^3/I^* , commonly known as the Poincaré dodecahedral space.

At the time of the publication of Weeks' AMS article [1], Weeks and his colleagues had only been able to compute the eigenmodes of S^3/I^* up to degree $m \leq 24$ due to accumulating round-off errors, meaning that they were only able to generate reliable estimates for the $\ell = 2, 3$, and 4 terms of the predicted CMB power spectrum. They used the $\ell = 4$ term to normalize, and the results that they obtained seemed extremely promising, with the predicted quadrupole and octupole matching observations. Additionally, the best fit was in the range $1.01 < \Omega < 1.02$, coinciding nicely with the WMAP estimate for the normalized density parameter.

The small number of free parameters associated with the dodecahedral space helped make this result especially satisfying. For example, while one can make a 3-torus from any one of 6 parallelepipeds, one can only make the dodecahedral space using a regular dodecahedron. Additionally, in most 3-manifolds the position of the observer will affect the predicted CMB power spectrum, but in the dodecahedral space, the spectrum will be unaffected by her position. Thus one can see how the dodecahedral space greatly reduces the number of free parameters as opposed to

other potential spaces. In fact, Ω was the only free parameter used in the study. Therefore, it seemed quite promising that the dodecahedral space model was able to predict quadrupole, octupole and density values that aligned so nicely with observations.

7 Do physical observations support the predictions of a dodecahedral model?

If the universe is indeed a Poincaré dodecahedron, then the following should hold true:

1. The low- ℓ terms in the CMB power spectrum should be weak.
2. Space should be slightly curved.
3. We should be able to see multiple images of the same source in the sky.

As has already been discussed, the WMAP satellite data produced a CMB power spectrum with a low quadrupole and octupole, so the first prediction coincides perfectly with observations. The second prediction, on the other hand, may or may not hold true. When Weeks' article was originally published [1], WMAP data suggested that $\Omega = 1.02 \pm 0.2$. The dodecahedral model requires space to be slightly curved (i.e. $\Omega \approx 1.02$), so the measurements for Ω were certainly consistent with a dodecahedral space, but at the same time they did not rule out the possibility of a flat universe with $\Omega = 1$. Since the publication of the article, NASA has released

additional and improved WMAP data, which may favor a flatter space. The 7-year WMAP data, released in January 2010, suggests that either $0.99 < \Omega < 1.01$ at the 95% confidence level or $0.99 < \Omega < 1.02$ at the 95% level, depending on which other data sets it is combined with [10]. While these new estimates for Ω do not rule out the possibility of a dodecahedral universe, they clearly diminish some of the support for the dodecahedral model.

What about the last prediction? If $\Omega = 1.02$, then the radius of a circle inscribed in the fundamental dodecahedron is a fair amount smaller than our horizon radius, implying that the fundamental dodecahedron is smaller than our horizon sphere. This being the case, the horizon sphere should “wrap around the universe and intersect itself.” That is, the horizon radius will exceed the injectivity radius and we will be able to see various points that are identified with each other. Because the intersection of two spheres is a circle, each self-intersection of the horizon sphere will be a circle and we, at the center of our horizon sphere, will be able to see the same circle of intersection on opposite sides of the sky. We can use CMB temperature fluctuations to look for such matching circles: identical density patterns will be reflected in identical temperature patterns. If we could find the matching circles predicted by a Poincaré dodecahedral space, we would have solid proof of the shape of our universe.

Unfortunately, a search performed by Cornish *et al* and using WMAP data looked for matching circles predicted by various topologies, including the dodecahedral space, but found none [11]. These results, although disheartening, do not

necessarily rule out the possibility of a compact universe. The CMB temperature fluctuations do not perfectly reflect density fluctuations due to various sources of contamination. For example, the temperature of the microwaves changes due to the Doppler effect, meaning that their wavelengths (and hence temperature) change as they move relative to us observers. Additionally, gravitational influences may have affected the radiation's temperature by causing them to lose energy during their 13.7 billion years of traveling toward us. While Cornish *et al* certainly attempted to control for contamination, their data still contained foreground contamination from the Milky Way and it is possible that this contamination was strong enough to obscure matching circles. It is always possible that improved techniques for removing foreground contamination may help researchers to find matching circles in the future.

Nevertheless, it is a topic of intense debate whether researchers will find the six sets of matching circles predicted by the dodecahedral model. Although researchers such as Boudewijn Roukema, arguing for a dodecahedral universe, have suggested that the sets of matching circles have indeed already been found [12], others have pointed out flaws in the methodology and, in fact, offered evidence that the dodecahedral model is not an apt model for our universe [13].

What if the matching circles do not exist? Such a scenario would certainly still leave open the possibility of a compact universe, although it would mean that our injectivity radius is comparable to or larger than our horizon radius. A universe about the same size as, or only slightly larger than, the horizon sphere, could still explain

the missing large scale fluctuations in the CMB power spectrum. If researchers are not able to find the desired matching circles, the hope is that the universe is not too much larger than the horizon sphere and that – in the same way that one can determine the length of a guitar string by observing vibrations on its middle 80% – we will be able to detect the topology of the universe using only what we can observe in our horizon sphere.

8 New evidence

In addition to the unexpectedly low quadrupole, the WMAP data shows an unusual quadrupole-octupole alignment [14]. Since the publication of Weeks' article, improved techniques for calculating eigenmodes have allowed mathematicians to investigate how well the dodecahedral model explains this additional mystery. Working with Jesper Gundermann's simulation of the CMB in S^3/I^* with modes up through degree $m = 102$, Weeks and Gundermann found the Poincaré dodecahedral space unable to explain any correlation between the quadrupole and octupole [14]. As Weeks points out, however, this does not serve as conclusive evidence against a dodecahedral universe: it is possible that the quadrupole-octupole alignment is the result of foreground contamination. Nevertheless, other spaces' ability to better explain the alignment may help to unmake the case for the Poincaré dodecahedral space. In response to the discovery of the anomalous alignment, Aurich *et al* explored the hyperbolic Picard space, the Poincaré dodecahedron, binary tetrahedron, binary octahedron, and the hypertorus [15]. All of these spaces suppress the low- ℓ

terms just as the dodecahedral space does, but none were found to fully explain the quadrupole-octupole alignment. Interestingly, though, out of all of these spaces, the Picard universe showed the greatest alignment between the quadrupole and octupole. Given that the recently released 7-year WMAP data estimate $\Omega = 1.0 \pm 0.01$ leaves more room for the possibility of a hyperbolic universe, this finding might stack some evidence against the case for a dodecahedral universe. If improved data ever begins to more strongly favor a hyperbolic universe, the Picard space may become a major candidate for further investigation.

However, the Picard space is not the only model for the universe competing against the Poincaré dodecahedral space. The so-called standard model predicts an infinite Euclidean universe and recently may have gained some additional support. When the first set of WMAP data was released, the observed temperature fluctuations in the CMB radiation did not match up well with those predicted by the standard model. The new 7-year WMAP data, however, seems to provide better support for the standard model. Not only does the new estimate for Ω of 1.0 ± 0.01 favor a Euclidean universe more strongly than the old estimate of $\Omega = 1.02 \pm 0.02$ did, but the standard model predicts specific patterns of polarization around hot and cold spots in the universe, and these patterns have now been observed in the 7-year data.

Perhaps, then, our universe is not spherical at all, but rather Euclidean or even hyperbolic. So are we back where we started, with no clue as to the topology of the universe? Not at all. Over the past two decades, different data sets have favored each

of the three types of manifolds under consideration: spherical, Euclidean and hyperbolic. But as mathematicians continue working with physicists and cosmologists to solve the mystery of the shape of our universe, they continue to develop sophisticated techniques to test complex models. In so doing, they continue increasing our understanding of spherical, Euclidean and hyperbolic spaces, providing theoretically testable hypotheses about what we should expect to observe in our universe given a particular manifold as a model. Moreover, even as particular hypotheses appear to be proven untrue, this work demonstrates the power of seemingly abstract topological models to describe real and meaningful properties of the physical universe. As data collection techniques and computational methods continue to improve, this seedbed of knowledge will undoubtedly help to nicely piece together otherwise cryptic physical observations in order to draw important conclusions about the nature of our universe.

9 Appendix A

As stated previously, one possible explanation for the low quadrupole value is that our universe has finite volume and is too small to support such long wavelengths. But if our universe is too small to support large-scale fluctuations, one may wonder why the quadrupole value was nonzero. If our universe is too small to support these wavelengths, then how did we observe any fluctuations on this scale?

To see how this is possible, we will examine a lower dimensional analogy. Suppose that instead of a 3-manifold, the universe was a 2-torus and that instead of a horizon sphere, we observed the CMB radiation within a horizon circle. If the horizon circle is a fair amount larger than our universe, within the horizon circle one will see various copies of the fundamental domain polygon. If we define the size of the fundamental domain polygon to be one unit, then the universe will not be able to support any fluctuations broader than one unit. However, in Figure 11, we see that larger-scale fluctuations can be observed: in our diagram, the copies of the fundamental domain polygon line up to create a streak of blue on the left side of the horizon circle that is approximately 3 units long, and a streak of red on the right side that is about 2 units long. Even though no one copy of the fundamental domain polygon can support a fluctuation broader than one unit, the alignment of the polygons allows for the detection of broader fluctuations. Clearly, then, some large-scale fluctuations can be observed in a small, finite-volume universe. However, we would expect to observe far fewer of these large-scale fluctuations in such a universe because on large angular scales any temperature fluctuations in the CMB would, for the most part,

tend to average out. Thus, in a small, finite-volume universe we would expect to see a low – but not necessarily zero – quadrupole value, which is exactly what the WMAP data showed.

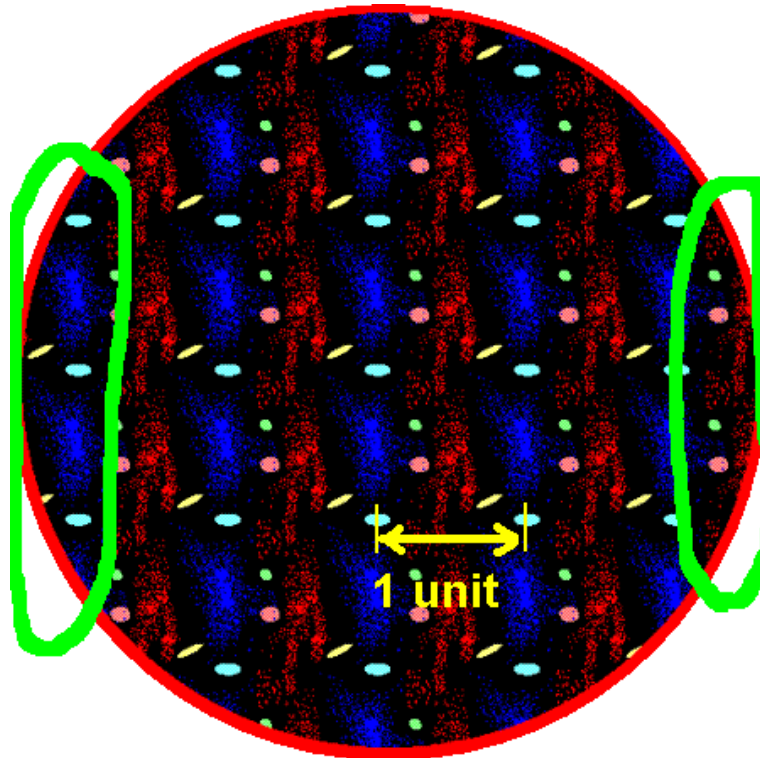


Figure 11: Although the size of the fundamental cell is only one unit, we observe a streak of blue on the left that is about 3 units long and a streak of red on the right that is about 2 units long. Figure courtesy of Jeffrey Weeks.

10 Appendix B

Theorem 10.1. (Some Properties of Homomorphisms) *Let ϕ be a homomorphism from a group G to a group F and let H be a subgroup of G . Then $\phi(H)$ is a subgroup of F . Also, if $|\text{Ker}\phi| = n$, then ϕ is an n -to-1 mapping from G onto $\phi(G)$.*

Theorem 10.2. (First Isomorphism Theorem) *Let ϕ be a group homomorphism from G to F . Then the mapping from $G/\text{Ker}\phi$, given by $g\text{Ker}\phi \mapsto \phi(g)$, is an isomorphism. In symbols, $G/\text{Ker}\phi \approx \phi(G)$.*

Theorem 10.3. (Cauchy's Theorem) *Let G be a finite group and let p be a prime that divides the order of G . Then G has an element of order p .*

Theorem 10.4. (Lagrange's Theorem) *If G is a finite group and H is a subgroup of G , then $|H|$ divides $|G|$.*

References

- [1] J. Weeks, *The Poincare dodecahedral space and the mystery of the missing fluctuations*, Notices of the AMS **51** (2004), no. 6, 610-619.
- [2] *Tests of big bang: the CMB*, http://map.gsfc.nasa.gov/universe/bb_tests_cmb.html.
- [3] J. Weeks, *The shape of space*, CRC Press, 2002.
- [4] J.P. Luminet, *The shape and topology of the universe*, www.arxiv.org/0802.2236.
- [5] J. Weeks, *Detecting topology in a nearly flat hyperbolic universe*, International Journal of Modern Physics (2008).
- [6] H. Groemer, *Geometric applications of Fourier series and spherical harmonics*, Cambridge University Press, 2009.
- [7] J. Gundermann, *Predicting the CMB power spectrum for binary polyhedral spaces*, www.arxiv.org/astro-ph/0503014.
- [8] J. Gallian, *Contemporary abstract algebra*, 7 ed., Brooks/Cole, 2006.
- [9] E. Gausmann, R. Lehoucq, J.P. Luminet, J.P. Uzan, and J. Weeks, *Topological lensing in spherical spaces*, Classical and Quantum Gravity **18** (2001), 5155-5186.
- [10] *WMAP cosmological parameters*, <http://lambda.gsfc.nasa.gov/product/map/dr3/parameters.cfm>.
- [11] N. Cornish, D. Spergel, G. Starkman, and E. Komatsu, *Constraining the topology of the universe*, Physical Review Letters **92** (2004), no. 20.
- [12] B. Roukema, *Does gravity prefer the Poincare dodecahedral space?*, International Journal of Modern Physics **18** (2009), no. 14.
- [13] J. Shapiro Key, N. Cornish, D. Spergel, and G. Starkman, *Extending the WMAP bound on the size of the universe*, Physical Review **75** (2007).

- [14] J. Weeks and J. Gundermann, *Dodecahedral topology fails to explain quadrupole-octupole alignment*, *Classical and Quantum Gravity* **24** (2007), 1863-1866.
- [15] R. Aurich, S. Lustig, F. Steiner, and H. Then, *Cosmic microwave background alignment in multi-connected universes*, *Classical and Quantum Gravity* **24** (2007), 1879-1894.
- [16] W. Thurston, *Three-dimensional geometry and topology*, Vol. 1, Princeton University Press, 1997.